J Solid State Electrochem (2001) 5: 562–567
DOI 10.1007/s100080000179

ORIGINAL PAPER

Xinming Qian · Dongqi Qin · Yubai Bai · Tiejin Li
Xinyi Tang · Erkang Wang · Shaojun Dong

Photosensitization of TiO_2 nanoparticulate thin film electrodes by CdS nanoparticles

Received: 23 March 2000 / Accepted: 9 October 2000 / Published online: 23 May 2001

Abstract Surface photovoltage spectra (SPS) measurements of TiO_2 show that a large surface state density is present on the TiO_2 nanoparticles and these surface states can be efficiently decreased by sensitization using CdS nanoparticles as well as by suitable heat treatment. The photoelectrochemical behavior of the bare TiO_2 thin film indicates that the mechanism of photoelectron transport is controlled by the trapping/detrapping properties of surface states within the thin films. The slow photocurrent response upon the illumination can be explained by the trap saturation effect. For a TiO_2 nanoparticulate thin film sensitized using CdS nanoparticles, the slow photocurrent response disappears and the steady-state photocurrent increases drastically, which suggests that photosensitization can decrease the effect of surface states on photocurrent response.

Keywords Surface photovoltage spectra · Photoelectrochemistry · Photosensitization · TiO_2 and CdS nanoparticles · Thin film

Introduction

Photoelectrochemical cells (PEC) based on the photosensitization of semiconductor films with organic dyes [1, 2] and inorganic nanoparticles [3, 4, 5] are of great interest since Graetzel et al. [6] reported a PEC with power conversion efficiencies near to 10%. Very Recently, Graetzel et al. [7] reported a type of solar cell based on a dye-sensitized heterojunction of TiO_2 with an amorphous organic hole-transport material as the solid electrolyte. The innovation of the Graetzel-type cell includes two aspects: the first is the use of TiO_2 semiconductor films supported on conducting glass as photo-anodes, and the second is the use of ruthenium complexes as sensitizes whose absorption spectra overlap well with the solar emission spectrum [8]. Today, the most promising dye-sensitized system is based on a nano-structured network of TiO_2 [9], because other nano-crystalline semiconductor materials (SnO_2 [10], ZnO [11], Fe_2O_3 [12, 13]) do not equal the excellent characteristics of the anatase-based cells.

For efficient solar energy conversion, the dye is required to have high absorption coefficients over the whole spectral region from NIR to UV. However, only a very limited number of dyes give high photocurrent quantum yields and are reasonably stable against photodegradation [14]. Another interesting approach conducted in several laboratories [15, 16, 17] for achieving efficient charge separation involves the coupling of two semiconductor particles with different energy levels. The difference in energy levels of the two semiconductor systems plays an important role in achieving the efficient charge separation. This phenomenon was named ''semiconductor sensitization'' [18]. Several methods have been reported for the preparation of the thin sensitized layer such as electrodeposition, chemical solution deposition, and colloid coating [19]. As already pointed out, the ''semiconductor sensitization'' principally implies several advantages as compared to organic dyes. The system is thought to be of increased photo-stability with the magnitude of photocurrent, and especially, the band-gap and thereby the absorption range is easily adjustable by the size of the particles [20]. Since photogenerated electrons and holes can be separated effectively by semiconductor sensitization, this effect seems important to develop low-cost and efficient solar cells.

X. Qian · E. Wang · S. Dong (✉)
Changchun Institute of Applied Chemistry,
Chinese Academy of Sciences, Jilin,
Changchun 130022, P. R. China
E-mail: dongsj@ns.ciac.jl.cn
Tel.: +86-431-5689711
Fax: +86-431-5689711

D. Qin
College of Chemistry and Molecular Engineering,
Peking University, Beijing 100871, P. R. China

Y. Bai · T. Li · X. Tang
Department of Chemistry, Jilin University, Jilin,
Changchun 130023, P. R. China

For the electron transport in the thin film, several mechanisms have been suggested: a hopping type of mechanism [21], the possibility of a tunneling effect between the particles [22], and a diffusion model under steady state illumination [23]. In any case, trapping of conduction band electrons by surface states strongly influences the charge transport properties of those films. Accordingly, it is of interest to investigate the effect of surface states on photochemical properties. In this paper, we report on the fabrication and photoelectrochemical studies of nanometer TiO_2 thin films sensitized using CdS nanoparticles. The objective is to investigate the effect of semiconductor sensitization on the surface states of TiO_2. It is shown that the semiconductor sensitization has improved the separation and transfer kinetics of photocarriers and increased the photocurrent response.

Materials and methods

All substances were of analytical grade and used without further purification. Deionized water was used to prepare all solutions. The solutions were always prepared just before each experiment.

Preparation of TiO_2 nanoparticulate thin films

The TiO_2 nanoparticle sol [24] and its nanoparticulate thin films [25, 26] were prepared by the methods reported previously. A piece of 2×4 cm^2 conducting glass ITO (indium tin oxide, made by Asahi Glass Company of Japan, sheet resistance was 7Ω/square) was fixed on a glass plate, using adhesive tape covered on two parallel edges of ITO to control the thickness of the TiO_2 film and to provide an area for electrical contact. A small aliquot of the diluted TiO_2 colloidal suspension was applied to a conducing surface and dispersed with a glass rod sliding over the tape-covered edges then was dried in air at gradually elevating temperature. The TiO_2 colloid-coated glass plate was then sintered at 350 °C for 30 min, then a wire was attached to the conducting area with copper epoxy adhesive. The resulting electrode was mounted at the end of a glass tube. To prevent dark current through the electrode, the free area of the electrode was covered with epoxy resin. The resulting exposed area of the TiO_2 nanoporous film electrodes is 0.5 cm^2. The thin films are referred to as ITO-TiO_2 electrodes.

Modification with CdS nanoparticles

The method for modifying of ITO-TiO_2 films with CdS was similar to that described before [21]. The ITO-TiO_2 electrodes were dipped in a saturated solution of $Cd(NO_3)_2$ for 1 min, rinsed with water, dipped into 0.1 mol/L Na_2S solution for 1 min and finally rinsed with water again. The coating procedures were repeated five times because no significant increase in the absorption was seen when the CdS deposition was continued beyond five treatments [21]. The latter films are referred to as ITO-TiO_2/CdS electrodes.

Characterization of TiO_2 particle powder, ITO-TiO_2 and ITO-TiO_2/CdS electrodes

The details of the characteristics of TiO_2 colloid can be found elsewhere [24]. SPS measurements were carried out with a home-built apparatus that had been described in our previous papers [26, 27, 28]. Electric field induced surface photovoltage spectroscopy (EFISPS) is a technique that combines the field-effect principle with SPS. The typical structure of a sample cell for SPS measurements is a sandwich structure, and the samples are installed between ITO electrodes. For EFISPS, the external electric field is applied to the two sides of sample and is regarded as positive when the side under illumination is connected to a positive electrode.

Photoelectrochemical measurements

The electrochemical and photoelectrochemical properties were performed in a standard three-compartment cell with a quartz window, consisting of a Pt plate counter electrode and a saturated calomel electrode (SCE) as reference electrode in 0.5 mol/L Na_2SO_4 solution. The voltammetry experiments were performed with EG & G PAR Model 173 potentiostat, driven by a Model 175 universal programmer. The photocurrent-time profile experiments were carried out with a PAR M5206 lock-in amplifier. As a light source, a 200 W xenon lamp was used.

Results and discussion

Characterization of UV-V is absorption

The absorption spectra of a TiO_2 colloid suspension in water (spectrum a), ITO-TiO_2 (spectrum b), and ITO-TiO_2/CdS electrode (spectrum c) are shown in Fig. 1. The inset figure is the XRD pattern of TiO_2 powder. Using the Debye-Scherrer equation, the crystallite size of TiO_2 is calculated to be 5 nm. Compared with the absorption in sol, the onset of the absorption for TiO_2 thin film exhibits a slight red shift, which suggests the aggregation of particles during the air-drying. As seen from the figure, the onset absorption for the TiO_2 sol is 360 nm, corresponding to the band gap of 3.44 eV. For ITO-TiO_2/CdS electrode, the photoresponse has been widened from the UV to the visible region. The red shift in the absorption onset of the ITO-TiO_2/CdS electrode indicates a decrease in the effective band gap similar to that of an organic dye sensitization system [8, 18]. The rapid decrease of the absorption around 320 nm was caused by ITO itself.

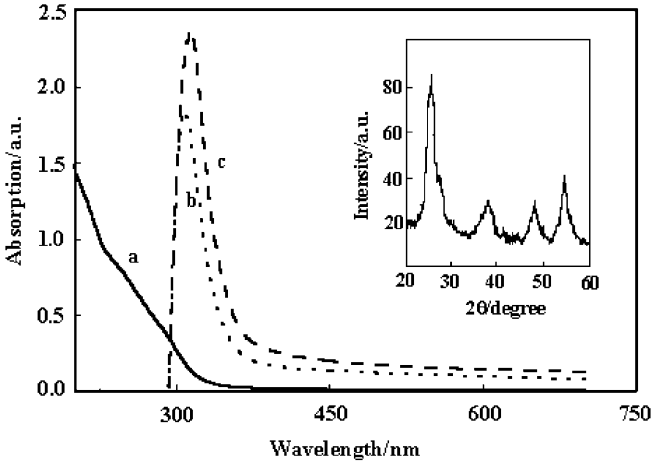

Fig. 1 Absorption spectra of (*a*) TiO_2 colloidal solution, (*b*) ITO-TiO_2 electrode, and (*c*) ITO-TiO_2/CdS electrode. The *inset figure* is the XRD pattern of TiO_2 powder

The results of SPS measurements

Fig. 2 and Fig. 3 show the SPS and EFISPS of TiO_2 powder before sintering treatment and of the ITO-TiO_2 electrode sintered at 350 °C for 30 min, respectively. With no external bias as presented in Fig. 2a and Fig. 3a, the strong SPS response peaks at 330 nm, with a threshold of 360 nm, can be attributed to the electronic transition from valance band to conduction band of TiO_2 ($O_{2p} \rightarrow Ti_{3d}$).

When the experiments were performed under a negative bias, the SPS response of TiO_2 powder before sintering treatment exhibited two important features. One is the increased SPS response relative to the band-band transition of TiO_2 at about 330 nm. The other is a wide photovoltage response between 350 nm and 800 nm with the peak position at 400 nm (Fig. 2, b), which can be assigned to the electronic transition from a valance band to the surface states of the TiO_2 nanoparticles. Hence, the wide, intensive SPS response indicates that a high density of surface states exists on the sample [29]. Previous spectroelectrochemical and voltammety measurements have also suggested that a density of intraband surface states of $(1–4)\times10^{17}$ m^{-2}, corresponding the 100–400 states per colloidal particles, attributed to coordinately unsaturated Ti^{3+} centers [30, 31], Ti-OH [32], and Ti-O^- [33]. When the experiments were performed under a positive bias, the SPS of TiO_2 powder before sintering treatment also exhibited two peak responses (Fig. 2, c). One is at 330 nm, corresponding to the band-band transition. The other is at 420 nm with an inversion the SPS response, which is relative to the intra-band transitions associated with the surface states. Because the surface states have more localized characteristics, the SPS response relative to surface states appears only under a suitable external bias.

As we know, the surface state bands can act as traps for photo-induced electrons and then prohibit the electron transfer process. To obtain a high photoelectric conversion efficiency, the number of the surface states should be decreased. In Fig. 3, b and Fig. 3, c, for the TiO_2 with heat treatment at 350 °C for 30 min, the photovoltage responses corresponding to the surface state transition are weakened. It is suggested that a suitable heat treatment can efficiently decrease the surface state density on TiO_2 nanoparticles.

For the TiO_2 thin film sensitized by CdS nanoparticles, the SPS response with no external bias shows two strong response peaks, with about the same intensity, at 330 nm and 400 nm separately resulting from the band-band transition of TiO_2 and CdS layers, respectively, in the ITO-TiO_2/CdS electrode (Fig. 4, a). This SPS response can be understood by use of an energy band model of the TiO_2/CdS double-layer as shown in Fig. 5. In this model, there is a heterojunction formed between the TiO_2 layer and the CdS layer, while there is a Shottoky junction at the TiO_2/CdS interface. When the ITO-TiO_2/CdS was irradiated with the light of 400 nm, the electrons in the valance band of CdS were excited to its conduction band. Flowing though the TiO_2/CdS

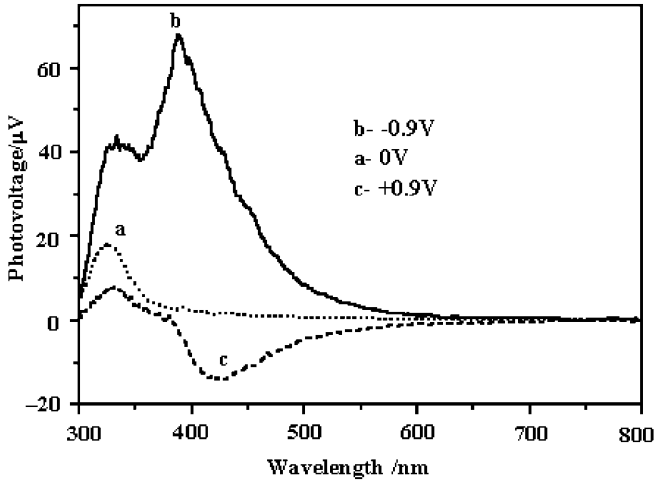

Fig. 2 SPS and EFISPS of TiO_2 powder before sintering treatment (*a*) 0 V, (*b*) –0.9 V and (*c*) +0.9 V

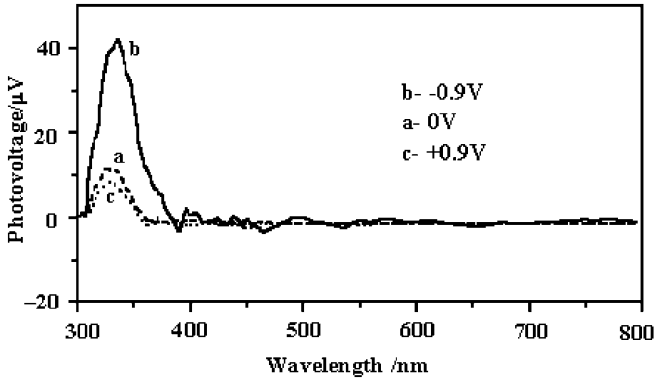

Fig. 3 SPS and EFISPS of TiO_2 thin film sintered at 350 °C for 30 min. (*a*) 0 V, (*b*) -0.9 V and (*c*) +0.9 V

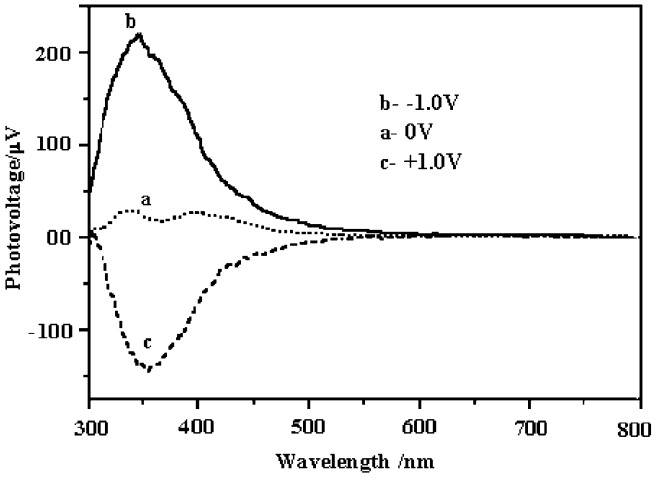

Fig. 4 SPS and EFISPS of TiO_2 thin film sensitized using CdS nanoparticles (*a*) 0 V, (*b*) –1 V and (*c*) +1 V

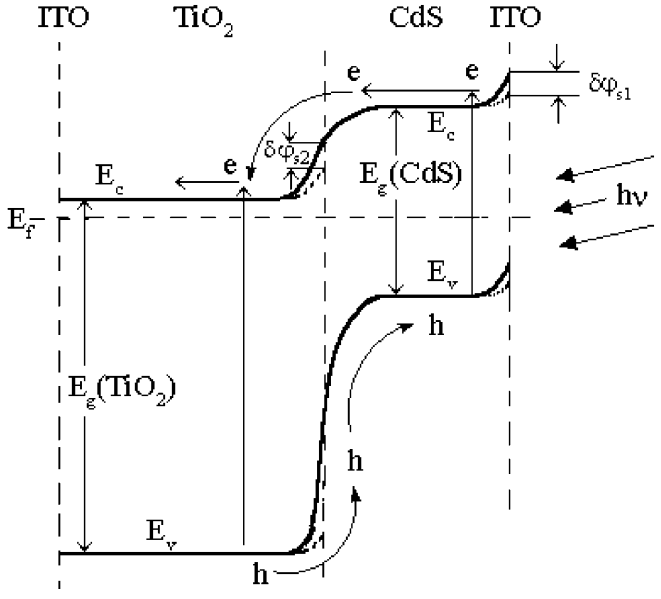

Fig. 5 The energy band model of TiO_2/CdS interface

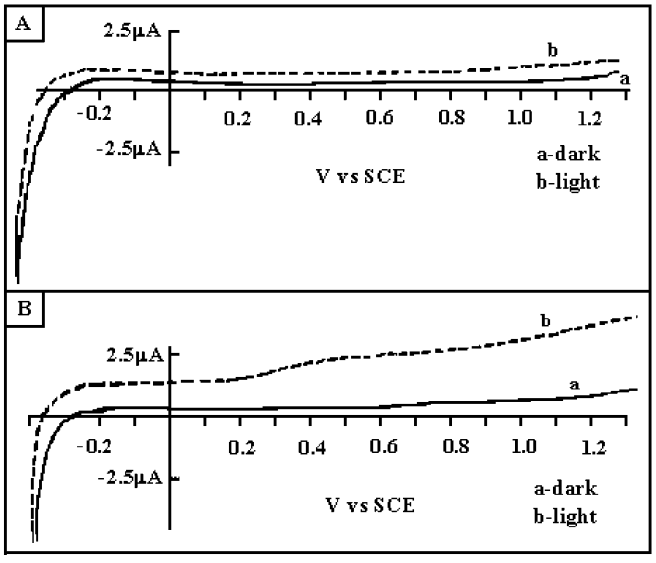

Fig. 6 Linear scan voltammograms of **A**: ITO-TiO_2, and **B**: ITO-TiO_2/CdS electrodes in 0.5 mol/L Na_2SO_4 solution *a* in the dark, and *b* under illumination with white light

interface, the electrons moved along the conduction band of TiO_2 and then arrived at the dark ITO surface, leading to the SPS response of CdS ($\delta\varphi_{s1}$). When the light was scanned to 330 nm, TiO_2 was also excited. The photo-induced electrons moved along its own conduction band to the dark ITO surface, while the holes passed through the TiO_2/CdS junction and moved into the valance band of CdS, resulting in the SPS response of TiO_2 ($\delta\varphi_{s2}$).

When the external electric field was applied on the ITO-TiO_2/CdS electrode, both of the two SPS responses were increased together with a strongest photovoltage response peak appeared at about 355 nm (Fig. 4, b and Fig. 4, c). This strongest SPS response indicates the sums of the photo-responses of the two semiconductor layers. Another interesting phenomenon is the only small SPS response between 350 nm and 800 nm existing relative to the surface states under the external bias, which suggests that the semiconductor sensitization also can decrease the surface state density on nanoparticles. Thus, the semiconductor sensitization as well as the heat treatment is an efficient method to decrease the surface state density on nanoparticles.

Photoelectrochemial properties

(a) The linear scan voltammetry characteristics

The linear scan voltammetry characteristics of ITO-TiO_2 and ITO-TiO_2/CdS electrodes were obtained by registering current at controlled potentials under dark and illumination conditions [35, 36]. Fig. 6A and Fig. 6B show the linear scan voltammograms of ITO-TiO_2 and ITO-TiO_2/CdS electrodes, respectively, in 0.5 mol/L Na_2SO_4 solution. Several important features of Fig. 6A need to be emphasized. The amount of dark current in the cathodic region is very high, which can be attributed to the electrolysis of water (Fig. 6A-a). Under illumination the photocurrent of ITO-TiO_2 appears at –0.38 V vs. SCE, then increases with increasing anodic potential and approaches a saturation limit at approximately –0.2 V (Fig. 6A-b). Another interesting behavior of the I-V characteristics is the observation of a zero photocurrent at a potential around –0.38 V, which is close to the earlier reported value of –0.35 V [19]. This potential corresponds to the flat-band potential of an n-type semiconductor. Assuming that the flat-band potential gives roughly the same response as the energy level of the bottom of the conduction band, the conduction band potential of the TiO_2 studied here is assumed to be –0.38 V. Then the valence band edge can be estimated by applying the determined energy gap to the conduction band edge.

In Fig. 6B, the enhancement of the photocurrent generation can be seen for the ITO-TiO_2 electrode modified with CdS nanoparticles, which demonstrates the cascading flow of electrons from the excited CdS to TiO_2 and then to the collecting surface of ITO.

The mechanism of photocurrent generation in the ITO-TiO_2/CdS modified electrode is illustrated in Fig. 7. CdS is a short band gap semiconductor ($E_g = 2.5$ eV) with its conduction band being –0.73 vs. SCE, more negative than that of TiO_2 (–0.38 eV vs. SCE), as obtained from above linear scan voltammetry measurement under illumination. Since the CdS thin film covers the surface of TiO_2, the photoelectrochemical property will be governed by the CdS layer.

Upon optical excitation of CdS, the photogenerated electrons quickly transfer to TiO_2, while holes accumulate at the CdS surface. The electron transfer across

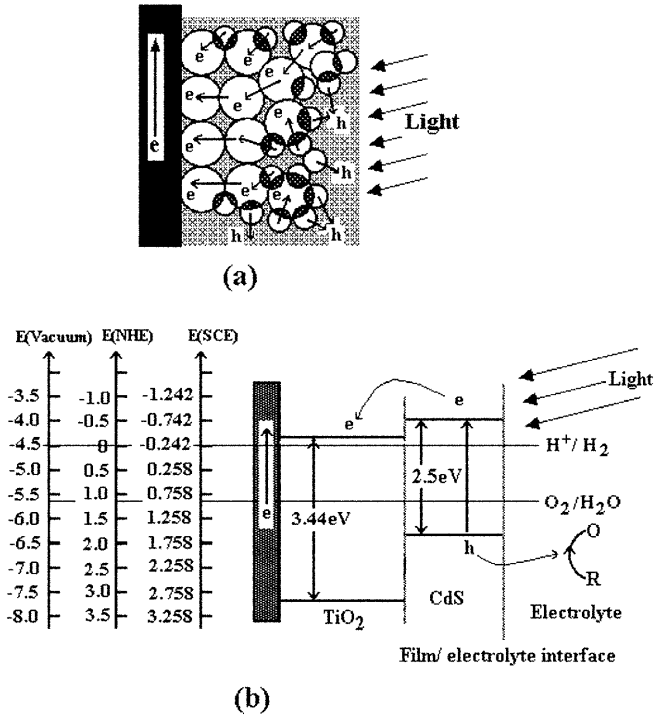

Fig. 7 Mechanism of photocurrent generation in ITO-TiO_2/CdS electrode **a** schematic diagram illustrating the charge separation in ITO-TiO_2/CdS electrode, and **b** schematic diagram for energy levels of TiO_2/CdS semiconductors in electrolyte

a colloidal heterojunction between CdS and TiO_2 occurs in less than 500 fs [37]. This value illustrates how fast the electron transfer processes from nanometer semiconductors can be expected to be. If the holes quickly reached the surface and reacted with a species in the electrolyte, the excited electrons left behind would be accumulated in the conduction band of TiO_2. In this case, the driving force causing the electrons to move in the direction toward the back-contact is the sum of the electrostatic repulsion and the concentration gradient of the excited electrons in TiO_2 film [38]. Since this gradient is not an ideal type of Schottky barrier, significant loss of electrons is encountered during the transport because of recombination at the grain boundaries. At the interface, one can expect the interaction between TiO_2 and CdS particles and the formation of a thin junction of Ti-Cd-S. The existence of such a junction would improve the process of charge separation by providing the necessary energy gradient for the flow of electrons to TiO_2 particles [38]. This will decrease the recombination at the interface formed between CdS and TiO_2 and decrease the effect of the surface state density of TiO_2 on the photocurrent response. With the charge recombination greatly suppressed, the lifetime of photo-induced carriers is increased significantly, so that higher concentration of photoelectrons moved to the ITO back contact can be obtained, so causing the increased photocurrent response.

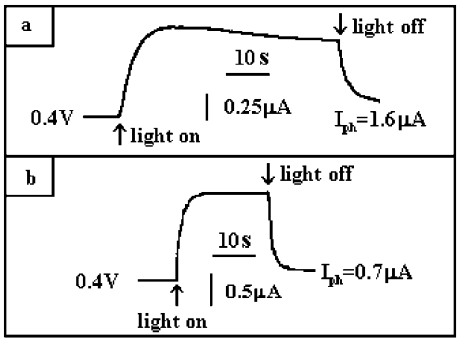

Fig. 8 Transient photocurrent response of **a**: ITO-TiO_2, and **b**: ITO-TiO_2/CdS electrodes at +0.4 V in 0.5 mol/L Na_2SO_4 solution under illumination with white light

(b) Transient photocurrent response

To give further credence to the effect of semiconductor sensitization on photocurrent response, the photocurrent-time profiles of ITO-TiO_2 and ITO-TiO_2/CdS electrodes were also measured. Fig. 8 shows the photocurrent-time characteristics of ITO-TiO_2 and ITO-TiO_2/CdS in 0.5 mol/L Na_2SO_4 solution at a constant potential.

With the light switching on and switching off, for the ITO-TiO_2 electrode (Fig. 8, a), the signs of the current change slowly. The electron trapping at the surface state appears to be responsible for the slow photocurrent response [39]. Upon the illumination, the shallow traps lying close to the conduction band are filled firstly by the conduction band electrons. The electrons trapped in the shallow surface states are expected to be released constantly from and retrapped into the deep surface states. Kang and coworkers [40] located the shallow surface states and the deep surface states to be 0.1 eV–0.6 eV and 1.3 eV–1.7 eV below the conduction band edge, respectively, as estimated from the fluorescence spectra. During the trapping-releasing-retrapping into deep surface states period, only a part of the photoelectrons including the released from shallow surface states can transport to the back-contact the electrode ITO, which shows the slowly increasing photocurrent response. This phenomenon was referred to as "trap saturation effects" [41]. Similarly, the slow response of the photocurrent decay to zero when the light is switched off is controlled by charge-carrier release from the traps.

However, for the ITO-TiO_2/CdS electrode (Fig. 8, b), the slow photocurrent response disappears and a dramatically increased steady-state photocurrent occurs in the anodic region. All these features suggest that semiconductor sensitization has a beneficial effect in improving the stability of the photocurrent and diminishing the trapping and detrapping of the surface states. The results obtained here are in accord with the discussion on the SPS response about the effect of the semiconductor sensitization on surface state density.

Conclusion

The SPS measurements show that a large surface state density is present on the TiO_2 nanoparticles and that these surface states can be efficiently decreased by selecting suitable heat treatment and nanoparticle sensitization. Both the photocurrent response and the charge recombination kinetics in TiO_2 thin films are strongly influenced by trapping/detrapping of surface states. The slow photocurrent response upon illumination is attributed to trap saturation effects. When the TiO_2 thin film electrode has been sensitized using CdS nanoparticles, the slow photoresponse disappears and the steady-state photocurrent value increases drastically. All the results suggest that the TiO_2 thin film sensitized by CdS can achieve a better charge separation and provide a simple alternative to minimize the effect of surface states on the photocurrent response.

Acknowledgements This work was supported by National Natural Science Foundation of China (No. 20075028 and No. 20073016), China Postdoctoral Science Foundation, and K. C. Wang Postdoctoral Research Award Fund of Chinese Academy of Science. The authors gratefully acknowledge Prof. Shengmin Cai (Department of Chemistry, Peking University, Beijing) for allowing us free use of their electrochemical facilities and technical assistance.

References

1. O'Regan B, Schwartz DT (1998) Chem Mater 10:1501
2. Kamat PV, Bedja I, Hotchandani S, Patterson LK (1996) J Phys Chem 100:4900
3. Nasr C, Kamat PV, Hotchandani S (B 1998) J Phys Chem 102:10047
4. Khan SUM, Akikusa J (1998) J Electrochem Soc 145:89
5. Hoyle R, Sotomayor J, Will G, Fitzmaurice D (1997) J Phys Chem 101:10791
6. O'Regan B, Graetzel M (1991) Nature 353:737
7. Bach U, Lupo D, Comte P, Moser JE, Weissortel F, Salbeck J, Spreitzer H, Graetzel M (1998) Nature 395:583
8. Hagfeldt A, Graetzel M (1995) Chem Rev 95:49
9. Barbe CJ, Arendsc F, Comte P, Jirousek M, Lenzmann F, Shklover V, Graetzel M (1997) J Am Ceramic Soc 80(12):3157
10. Vinodgopal K, Bedja I, Kamat PV (1996) Chem Mater 8:2180
11. Rensmo H, Keis K, Lindstrom H, Sodergren S, Solbrand A, Hagfeldt A, Lindquist SE, Wang LN, Muhammed M (1997) J Phys Chem 101:2598
12. Qian XM, Zhang XT, Ai X, Hao YZ, Liu FQ, Cai SM, Bai YB, Li TJ, Tang XY, Yao JN (1999) Mol Cryst & Liq Cryst 337:437
13. Qian XM, LU HH, Zhang XT, Li YS, Bai YB, Li TJ, Tang XY (1999) Acta Scientiarum naturalium Universitatics Jilinensis 4:87
14. Vogel R, Pohl K, Weller H (1990) Chem Phys Lett 174:241
15. Matsumoto H, Matsunaga T, Skata T, Mori H, Yoneyama H (1995) Langmuir 11:4283
16. Fitzmaurice D, Frei H, Rabani J (1995) J Phys Chem 99:9176
17. Rogers KD, Painter JD, Healy MJ, Lane DW, Ozsan ME (1999) Thin Solid Films 339:299
18. Kohtani S, Kudo A, Sakata T (1993) Chem Phys Lett 206:166
19. Torimoto T, Nagakubo S, Nishizana M, Yoneyama H (1998) Langmuir 14:7077
20. Vogel R, Hoyer P, Weller H (1994) J Phys Chem 98:3183
21. Konenkamp R, Henniger R, Hoyer P (1993) J Phys Chem 97:7328
22. Hoyer P, Weller H (1995) J Phys Chem 99:14096
23. Wahl A, Augustynski J (1998) J Phys Chem 102:7820
24. Zhao JZ, Wang ZC, Liu YH, Wang LW, Song Q, Yang H, Zhao MY (1999) Chem J Chinese Universities 20:467
25. Hao YZ, Yang MZ, Yu C, Cai SM, Liu MS, Fan LZ, Li YF (1998) Solar Energy Materials & Solar Cells 56:75
26. Qian XM, Zhang XT, Bai YB, Li TJ, Tang XY, Wang EK, Dong SJ (2000) J Nanoparticle Research 2:191
27. Du H, Cao YA, Bai YB, Zhang P, Qian XM, Li TJ, Tang XY (B1999) J Phys Chem 102:2329
28. Wang DY, Cao YA, Zhang XT, Liu ZQ, Qian XM, Ai X, Liu FQ, Wang DJ, Li TJ, Tang XY (1999) Chem Mater 11: 392
29. Cao F, Oskam G, Searson PC, Stipkala JM, Heimer TA, Farzad F, Meyer GJ (1995) J Phys Chem 99:11974
30. Kay A, Humphrey-Baker R, Graetzel M (1994) J Phys Chem 98:952
31. Moser J, Punchihewa S, Infelta PP, Graetzel M (1991) Langmuir 7:3012
32. Hoffmann MR, Martin ST, Choi W, Bahnemann DW (1995) Chem Rev 95:69
33. Shiga A, Tsujiko A, Ide T, Yae S. Nakato Y (1998) J Phys Chem 102:6049
34. Hiesgen R, Meissner D (1998) Adv Mater 10:619
35. Hao EC, Qian XM, Yang B, Wang DJ, Shen JS (1999) Mol Cryst & Liq Cryst 337:181
36. Nasr C, Hotchandani S, Kamat PV, Das S, Thomas KG, George MV (1995) Langmuir 11:1777
37. Gopidas KR, Bohorque ZM, Kamat PV (1990) J Phys Chem 94:6435
38. Hotchandani S, Kamat PV (1992) J Phys Chem 96:6834
39. Qian X M, Song Q, Bai YB, Li TJ, Tang XY, Dong SJ, Wang EK (2000) Chem J Chinese Universities 21:295
40. Kang TS, Kim D, Kim KJ (1998) J Electrochem Soc 145: 1982
41. Schwarzburg K, Willig F (1991) Appl Phys Lett 58:2520